Biochimica et Biophysica Acta 1822 (2012) 1671–1681

Contents lists available at SciVerse ScienceDirect

Biochimica et Biophysica Acta

journal homepage: www.elsevier.com/locate/bbadis

Na^+ and K^+ ion imbalances in Alzheimer's disease

Victor M. Vitvitsky [a], Sanjay K. Garg [a,1], Richard F. Keep [b], Roger L. Albin [c,d], Ruma Banerjee [a,*]

[a] Department of Biological Chemistry, University of Michigan Medical School, Ann Arbor, MI 48109-0600, USA
[b] Department of Neurosurgery and Molecular and Integrative Physiology, University of Michigan Medical School, Ann Arbor, MI 48109-0600, USA
[c] Department of Neurology, University of Michigan Medical School, Ann Arbor, MI 48109, USA
[d] Veterans Administration Ann Arbor Health System and Geriatric Research, Education and Clinical Center, Ann Arbor, MI 48105, USA

ARTICLE INFO

Article history:
Received 29 February 2012
Received in revised form 11 July 2012
Accepted 12 July 2012
Available online 20 July 2012

Keywords:
Alzheimer's disease
Amyloid β
Astrocyte
Brain
Sodium
Potassium

ABSTRACT

Alzheimer's disease (AD) is associated with impaired glutamate clearance and depressed Na^+/K^+ ATPase levels in AD brain that might lead to a cellular ion imbalance. To test this hypothesis, $[Na^+]$ and $[K^+]$ were analyzed in postmortem brain samples of 12 normal and 16 AD individuals, and in cerebrospinal fluid (CSF) from AD patients and matched controls. Statistically significant increases in $[Na^+]$ in frontal (25%) and parietal cortex (20%) and in cerebellar $[K^+]$ (15%) were observed in AD samples compared to controls. CSF from AD patients and matched controls exhibited no differences, suggesting that tissue ion imbalances reflected changes in the intracellular compartment. Differences in cation concentrations between normal and AD brain samples were modeled by a 2-fold increase in intracellular $[Na^+]$ and an 8–15% increase in intracellular $[K^+]$. Since amyloid beta peptide (Aβ) is an important contributor to AD brain pathology, we assessed how Aβ affects ion homeostasis in primary murine astrocytes, the most abundant cells in brain tissue. We demonstrate that treatment of astrocytes with the Aβ 25–35 peptide increases intracellular levels of Na^+ (~2–3-fold) and K^+ (~1.5-fold), which were associated with reduced levels of Na^+/K^+ ATPase and the Na^+-dependent glutamate transporters, GLAST and GLT-1. Similar increases in astrocytic Na^+ and K^+ levels were also caused by Aβ 1–40, but not by Aβ 1–42 treatment. Our study suggests a previously unrecognized impairment in AD brain cell ion homeostasis that might be triggered by Aβ and could significantly affect electrophysiological activity of brain cells, contributing to the pathophysiology of AD.

1. Introduction

Alzheimer's disease (AD), the most prevalent form of dementia, is a neurodegenerative disorder characterized by the presence of neurofibrillary tangles, dystrophic neurites and senile plaques composed predominantly of amyloid beta peptide (Aβ) derived from the amyloid precursor protein [1]. Aβ is 37–43 amino acids in length and residues 25–35 in the Aβ peptide are the most toxic [2]. Among other biochemical aberrations, elevated levels of reactive oxygen species [3], impaired glutamate clearance [4], and depressed Na^+/K^+ ATPase levels [5] have been reported in AD brain. Also, a decrease in Na^+/K^+ ATPase activity and protein levels was observed in hippocampus of APP + PS1 transgenic mice, a model for AD [6]. These biochemical effects suggest changes in antioxidant capacity, glutamate-based neurotransmission and in membrane polarization–repolarization, processes interconnected at a single metabolic hub. We hypothesized that in AD, impairments in the interconnections extending across astrocytes and neurons linking sulfur metabolism to glutamate-based neurotransmission and ion homeostasis, propagate through this intercellular network and result in coordinated changes in redox and ion regulation affecting both cell types.

Astrocytes are organized in extensive networks poised to dynamically influence neuronal function. The metabolic dependence of neurons on astrocytes renders them vulnerable to astrocytic dysfunction, which can exacerbate neuronal damage under pathological conditions [7,8]. Glutathione (GSH) is a major antioxidant in brain whose synthesis is limited by the availability of cysteine [9]. The latter can be synthesized from methionine via the transsulfuration pathway, or derived from imported cystine, which is reduced subsequent to its transport. The twin transporters, x_C^- and X_{AG}^-, link GSH metabolism to the glutamate–glutamine cycle and connect in turn to Na^+/K^+ ATPase [10,11]. The X_{AG}^- system (also known as EAAT transporters) clears glutamate released during synaptic transmission using the sodium gradient in a process that translocates $3Na^+$ (in) and one K^+(out) for every glutamate that is imported into the cell [12].

Abbreviations: AD, Alzheimer's disease; Aβ, amyloid β peptide; CAβ42, levels of Aβ 1–42 peptide in CSF; Cb, cerebellum; CDR, clinical dementia rating; CSF, cerebrospinal fluid; FC, frontal cortex; MRI, magnetic resonance imaging; PC, parietal cortex; PIB, results of [^{11}C]-Pittsburgh B compound positron emission tomography imaging; Ptau181, CSF phospho-tau 181 levels; Tau, CSF tau levels

* Corresponding author at: Department of Biological Chemistry, University of Michigan Medical School, 3320B MSRB III, 1150 W. Medical Center Dr., Ann Arbor, MI 48109-5606, USA. Tel.: +1 734 615 5238; fax: +1 734 763 4581.
E-mail address: rbanerje@umich.edu (R. Banerjee).
[1] Current address: Department of Internal Medicine-Geriatric Medicine, University of Michigan, Ann Arbor, MI 48109, USA.

0925-4439/$ – see front matter © 2012 Elsevier B.V. All rights reserved.
doi:10.1016/j.bbadis.2012.07.004

Astrocytes exposed to Aβ show lower glutamate uptake than untreated controls [13,14] and have a disturbed redox status [15]. Oxidative modification and impaired functioning of GLT-1 have been reported in AD brain and in Aβ-treated synaptosomes [4]. Glutamate uptake activates the Na^+/K^+ ATPase, which works to normalize the resting transmembrane ion gradients. Protein levels and the activity of the Na^+/K^+ ATPase are reported to be lower in AD brains compared to age-matched controls [5]. The glutamate gradient in turn drives the x_C^- antiporter, which exchanges extracellular cystine for intracellular glutamate in a stoichiometric process [10]. Expression of this antiporter decreases in Aβ treated astrocytes [15]. In addition to using the transmembrane sodium gradient, which drives the transport of glutamate and other metabolites, astrocytes take up potassium ions released during the repolarizing phase of action potentials [16] and changes in the astrocytic membrane potential can influence neuronal firing rates [17].

Heterocellular coupling between astrocytes and neurons is indispensable for cycling glutamate, and for redox and ion balance. Impairment at one or more key network nodes in either cell type is expected to have pleiotropic consequences. While perturbations in astrocytic redox balance [15,18] and glutamate clearance [13,14] in response to Aβ have received some attention, little is known about the effects of Aβ on the astrocytic cation inventory, which might in turn influence ion conductance changes that underlie many aspects of neuronal function.

To test the hypothesis that impaired glutamate clearance and depressed Na^+/K^+ ATPase levels observed in AD brain are associated with Na^+ and K^+ imbalances, we analyzed Na^+ and K^+ levels in postmortem brain tissues of normal and AD individuals as well as in cerebrospinal fluid (CSF) of AD patients and matched controls. Significant ion imbalances were found in the cortical (Na^+) and cerebellar (K^+) specimens of AD brain but not in CSF of AD subjects, suggesting that the observed changes in tissue samples reflect changes in the intracellular pool. Mathematical modeling of the experimental data showed that the observed differences in ion concentrations between normal and AD brain tissues can be explained by a 2-fold increase in intracellular [Na^+] and a 8–15% increase in intracellular [K^+] in AD individuals. To assess whether Aβ might be responsible for the observed ion imbalance in brain cells, we analyzed the effect of Aβ on Na^+ and K^+ concentrations in cultured primary mouse astrocytes, which are the most abundant cell type in brain. We found that treatment of astrocytes with Aβ 25–35 increased intracellular [Na^+] (~2–3-fold) and [K^+] (~1.5-fold), which is similar to the increase in intracellular Na^+ and K^+ levels observed in brain tissues of AD individuals. Similar ion imbalances were observed in astrocytes treated with Aβ 1–40, but not with Aβ 1–42. We speculate that ion imbalance in AD brain might result at least in part, from ion imbalance in astrocytes, which, in turn, might be induced by Aβ. To our knowledge, this study provides the first evidence for significant perturbation of ion homeostasis in AD brain, which could be important for the pathophysiology of brain dysfunction in AD.

2. Materials and methods

2.1. Human brain and CSF samples

AD brain and age-matched control samples were from the Michigan Alzheimer's disease Research Center Brain Bank. AD samples were derived from clinically well-characterized individuals participating in a prospective brain collection program. At death, one hemisphere was cut into 1–1.5 cm coronal slabs and frozen rapidly over liquid N_2 vapor. The other hemisphere was fixed in 10% neutral buffered formalin and used for neuropathologic analysis. All specimens are reviewed by the same neuropathologist and diagnosis was established by the Reagan-NIA criteria [19]. Slabs were stored in heat-sealed freezer bags at −80 °C until the time of tissue use. Age, gender, and post-mortem delay matched control specimens were derived from individuals with no clinical history of neurologic disease and normal neuropathologic examinations. Slabs were warmed to −20 °C and blocks of frontal cortex, parietal cortex, and cerebellum were prepared. The collection of human brain tissues was approved by the University of Michigan Medical School Institutional Review Board. CSF samples from non-demented individuals (clinical dementia rating (CDR) 0) and those with very mild to moderate Alzheimer's dementia (CDR 0.5–2) [20] were obtained from the Washington University's Alzheimer's Disease Research Center. Data for CSF levels of Tau, Ptau181, and Aβ 1–42 and data for PIB binding were obtained from the Washington University Biomarker and Imaging Cores, respectively. Details of these procedures have been published previously [21].

2.2. Cell culture

U-87MG (human astrocytoma), Jurkat (human T cell leukemia) and HEK293 (human embryonic kidney) cells were obtained from ATCC. All transformed cell lines were cultured with 100% medium change in 6-well plates with 2 mL medium per well. The following media were used for cultures of transformed cell lines: EMEM (ATCC) for U-87 MG cells, DMEM (Invitrogen) for HEK 293 cells and RPMI-1640 (Invitrogen) for Jurkat cells. All media contained 10% normal FBS (Hyclone), 100 units/mL penicillin and 100 μg/mL streptomycin (Invitrogen).

2.3. Isolation and culture of murine astrocytes

Primary murine cortical astrocyte cultures were prepared from 1 to 2 day old Balb/C pups as described previously [22,23]. At the end of the third passage, cells were seeded in 6-well ($1–2\times10^6$ cells/well/2 mL) or 12-well (1×10^6 cells/well/1 mL) plates and used for experiments after two days. DMEM/F12 mixture containing 10% heat-inactivated FBS, 2 mM additional L-glutamine, 100 units/mL penicillin and 100 μg/mL streptomycin was used as a complete medium for astrocyte cultures. The purity of astrocytes was determined as described previously [23] and was ≥93%. The protocols used for handling animals were approved by the University Committee on Use and Care of Animals, University of Michigan.

2.4. Aggregation of Aβ peptide

The lyophilized forms of the triflouroacetate salt of the human Aβ 25–35, Aβ 1–40, Aβ 1–42, and the reversed Aβ 35–25 peptide (Bachem) were aggregated as described previously [24]. Briefly, Aβ was dissolved in sterile double-distilled water as a 2 mM stock solution, incubated for 8 days at 37 °C and stored in aliquots at −80 °C. Formation of aggregates was evident from the turbidity of the solution and by observation under a light microscope.

2.5. Aβ treatment of cell cultures

U-87MG and HEK 293 cells were used for experiments at 80–90% confluency. Jurkat cells were used at a cell density of 2×10^6 cells/well. At the beginning of each experiment, 100% medium was changed and aggregated Aβ 25–35 was added to a final concentration of 50 μM (concentration estimated prior to aggregation). Cells were collected for ion analysis after 24 h of incubation with Aβ as described below.

Astrocytes were treated acutely or repeatedly with Aβ 25–35 and Aβ 35–25. Aβ 1–40 and Aβ 1–42 were only used in acute treatments. A single bolus of Aβ was added for acute treatment and samples were collected 24 h later. For the repeated treatment model, Aβ was added 3 times at 72 h intervals and samples were collected 24 h after the last treatment. Each time, Aβ was added to astrocytes after 100% change of the complete medium. In each independent experiment (using different preparations of astrocytes), cells were cultured in

2–3 wells in parallel for each experimental condition. Sample from each well was prepared and analyzed separately and the data were averaged. Cell death was observed in <10% of cells in culture following acute or repeated Aβ treatment and was comparable to that seen in the control cell culture as reported previously [15]. Cell death was monitored by the PI-AV labeling kit (BioVision) and the TUNEL assay kit (Roche) according to the vendor's protocols (data not shown).

Ouabaine (500 μM), aspartate β-hydroxamate (400 μM), furosemide (2 mM), bumetanide (10 μM), and dimethyl amiloride (50 μM) (Sigma) when used, were added to astrocytes exposed to repeated treatment with 50 μM Aβ 25–35 at the time of the last Aβ treatment, and cells were collected for ion analysis 24 h later.

2.6. Metabolite analysis

Frozen brain tissue (~100 mg) was pulverized in liquid N_2 and the resulting powder (~50 mg) was added to pre-weighed tubes containing 300 μL of 6% TCA (to precipitate protein) for glutamine and methionine analysis or 300 μL of metaphosphoric acid solution (16.8 mg/mL HPO_3, 2 mg/mL EDTA and 9 mg/mL NaCl, to precipitate protein) for glutamate analysis. The tubes were weighed again to determine the wet weight of the added tissue and then stored at −80 °C until further analysis. CSF samples were mixed with an equal volume of 10% TCA or metaphosphoric acid solution and stored at −80 °C until further analysis.

Glutamate concentration in CSF and brain samples was measured by HPLC with 2,4-dinitrofluorobenzene derivatization initially described for thiol analysis [25]. Concentrations of glutamine and methionine were measured by HPLC using *o*-phthaldialdehyde derivatization [25].

2.7. Western blot analysis

Astrocytes were collected for Western blot analysis after 24 h of acute treatment or the last repeated treatment with 50 μM of Aβ 25–35. Samples were prepared as described previously [26]. Antibodies against GLAST (EAAT1) (Millipore), GLT-1 (Santa Cruz Biotech), Na^+/K^+ ATPase α1 (Santa Cruz Biotech) and actin (Sigma) were used to monitor expression of the respective protein antigens and were detected using the Dura chemiluminescent horseradish peroxidase system (Pierce) according to the vendor's protocol. For quantification of Western blot data, the integrated intensity of protein band of interest was measured using ImageJ software and normalized to the integrated intensity of the actin band in the same samples.

2.8. Measurement of cations

Frozen brain samples (~100 mg) were added to a pre-weighed plastic tube containing 300 μL of deionized water, and the tubes re-weighed. Tissue was homogenized with a plastic pestle on ice, centrifuged at 15,000×*g* for 5 min and the supernatant was used for Na^+ and K^+ ion analysis using a flame photometer. CSF samples were used for ion analysis without any modifications. To analyze Na^+ and K^+ in cells pre-exposed to Aβ, culture medium was aspirated and stored frozen until analysis of the ions in the medium. Cells were washed twice with cold choline chloride solution (150 mM), and re-suspended in 100 μL of choline chloride solution. The cell suspension was freeze–thawed 3 times, cell membranes were removed by centrifugation and ion concentrations in the resulting supernatant were measured using a flame photometer. To measure protein concentration, ~30 μL of the cell suspension was mixed with an equal volume of lysis buffer and protein content was measured using the Bradford method as described previously [25]. The resulting ion concentrations were normalized to protein concentration in the cell suspension or normalized to the amount of tissue and presented as mmoles per g of protein or mmoles per kg of tissue, respectively.

2.9. Mathematical model for correlating total, intracellular and extracellular brain [Na^+] and [K^+]

To estimate intracellular concentrations of Na^+ and K^+ in brain samples using total (measured) concentration of ions in the tissue, we developed the following model.

Total tissue concentrations of Na^+ and K^+ are described by Eqs. (1) and (2) for mass conservation:

$$Na_t = (Na_{in}V_{in} + Na_{ex}V_{ex})/(V_{in} + V_{ex}) \quad (1)$$

$$K_t = (K_{in}V_{in} + K_{ex}V_{ex})/(V_{in} + V_{ex}). \quad (2)$$

Here Na_t and K_t denote total (measured) Na^+ and K^+ concentrations in tissue, Na_{in}, Na_{ex}, K_{in}, and K_{ex} denote intracellular and extracellular Na^+ and K^+ concentrations respectively, and V_{in}, and V_{ex} denote cell volume and extracellular volume in the tissue. The cell volume includes total volume occupied by all cells in the tissue sample and extracellular volume includes all extracellular compartments (interstitial liquid, CSF, blood plasma, *etc.*) in the sample.

For unit volume ($V_{in} + V_{ex} = 1$), Eqs. (1) and (2) transform to the following form:

$$Na_t = (Na_{in}V_{in} + Na_{ex}(1-V_{in}) = Na_{ex} + (Na_{in}-Na_{ex})V_{in} \quad (3)$$

$$K_t = (K_{in}V_{in} + K_{ex}(1-V_{in}) = K_{ex} + (K_{in}-K_{ex})V_{in}. \quad (4)$$

Here V_{in} and V_{ex} are fractions of the tissue volume corresponding to cell and extracellular volumes.

Eqs. (3) and (4) indicate that total tissue concentrations of Na^+ and K^+ are linear functions of the relative cell volume. As a consequence, the total K^+ concentration in samples of the same tissue with different relative cell volumes must be a linear function of total Na^+ concentration. These equations show that if intracellular and extracellular ion concentrations are constant, then an increase in the cell volume fraction in a tissue causes a linear decrease in total (measured) Na^+ concentration (because $Na_{in} - Na_{ex} < 0$), and a linear increase in total (measured) K concentration (because $K_{in} - K_{ex} > 0$).

Next, using Eq. (3) one can express V_{in} as a function of Na_t:

$$V_{in} = (Na_t - Na_{ex})/(Na_{in} - Na_{ex}). \quad (5)$$

By replacing V_{in} in Eq. (4) with the function in Eq. (5), we obtain the following equation:

$$\begin{aligned} K_t &= K_{ex} + (K_{in}-K_{ex})(Na_t - Na_{ex})/(Na_{in} - Na_{ex}) \\ &= K_{ex} + ((K_{ex}-K_{in})Na_{ex} + (K_{in}-K_{ex})Na_t)/(Na_{in} - Na_{ex}). \end{aligned} \quad (6)$$

This equation reveals the linear dependence of total K^+ concentration on total Na^+ concentration in tissue samples if intracellular and extracellular Na^+ and K^+ concentrations are constant and the cell volume fraction in samples varies. Eq. (6) can be rewritten in the following form:

$$K_t = A + B * Na_t \quad (7)$$

$$A = K_{ex} + (K_{ex}-K_{in})Na_{ex}/(Na_{in} - Na_{ex}) \quad (8)$$

$$B = (K_{in}-K_{ex})/(Na_{in} - Na_{ex}). \quad (9)$$

Eqs. (6)–(9) can be used to estimate intracellular tissue Na^+ and K^+ concentrations using total concentrations of Na^+ and K^+.

2.10. Statistical analyses

Statistical analysis and linear fits of experimental data were done using Origin 7 software (OriginLab). Comparison between groups was done using Student's *t* test. $p \leq 0.05$ was considered as the criterion for significant difference.

3. Results

3.1. Ion imbalances in AD brain

Tissue Na^+ and K^+ concentrations were determined in human postmortem brain samples of frontal cortex, parietal cortex, and cerebellum from 16 AD subjects and 12 age-matched controls (Table 1). On average, frontal and parietal cortical regions from AD subjects were found to exhibit significantly higher tissue Na^+ concentrations, while cerebellum, a region with lower amyloid pathology, exhibited a non-significant trend towards higher tissue Na^+ concentrations (Table 2). The average K^+ concentrations in frontal and parietal cortex samples of AD patients were not significantly different from K^+ concentrations in similar samples of control individuals, while K^+ concentrations in cerebellum samples of AD patient were significantly increased (Table 2). Differences in ion concentrations between AD and healthy subjects did not correlate with sex, age and postmortem time of the individual specimens (Table 1, Fig. S1).

In principle, the observed elevation in Na^+ concentration in AD brain samples could reflect increases in Na^+ concentration of either the intra- or the extra-cellular (blood, CSF, interstitial) compartment or an increase in the relative size (*i.e.* volume) of the extracellular (Na^+-rich) compartment. An increase in the relative extracellular volume has been reported in a mouse AD model [27]. To assess whether ion concentrations change in the extracellular compartment of AD brain tissue, we analyzed Na^+ and K^+ concentrations in CSF samples from clinically characterized AD subjects and matched controls (Table 3). No difference in Na^+ or K^+ concentrations between the two groups was observed (Table 3). Also, no difference in CSF Na^+ or K^+ concentrations was observed between males and females (Table S1). Thus, the increase in Na^+ in AD post-mortem tissue samples (Table 2) likely does not reflect changes in the composition of the

Table 2
Average ion and metabolite concentrations in brain samples from AD patients and age-matched controls.[a]

Parameter	Subjects	Frontal cortex	p	Parietal cortex	p	Cerebellum	p
Sodium (mmol/kg tissue)	Normal	73.9 ± 11.2	0.01	71.1 ± 8.0	0.01	68.9 ± 11.5	0.05
	AD	92.1 ± 20.8		85.0 ± 14.9		79.4 ± 14.6	
Potassium (mmol/kg tissue)	Normal	60.7 ± 8.0	0.38	63.7 ± 6.5	0.46	68.4 ± 10.0	0.02
	AD	57.7 ± 9.2		66 ± 9.2		76.2 ± 7.4	
Glutamine (mmol/kg tissue)	Normal	6.82 ± 3.99	0.82	6.98 ± 3.98	0.82	7.99 ± 2.63	0.78
	AD	6.57 ± 1.76		7.29 ± 2.96		8.26 ± 2.43	
Glutamate (mmol/kg tissue)	Normal	9.0 ± 1.7	0.08	9.2 ± 1.6	0.13	10.9 ± 3.4	0.68
	AD	10.5 ± 2.6		10.7 ± 2.9		11.4 ± 3.0	
Methionine (μmol/kg tissue)	Normal	231 ± 93	0.56	257 ± 97	0.54	474 ± 244	0.01
	AD	204 ± 132		305 ± 257		262 ± 105	

[a] The number of samples in each group was as follows: AD (n = 16) and controls (n = 12) and the data represent the mean ± SD.

Table 1
Postmortem $[Na^+]$ and $[K^+]$ values in brain tissue of normal individuals and AD patients.

Patient ID	Diagnosis	Sex	Age (years)	Postmortem time (h)	[Na] (mmol/kg tissue)			[K] (mmol/kg tissue)		
					FC[a]	PC	Cb	FC	PC	Cb
1	Normal	M	91	8	61.7	72.0	73.2	63.5	74.1	63.5
2	Normal	F	86	18	76.0	82.8	59.5	58.4	62.7	76.4
3	Normal	F	95	18	69.4	61.5	81.0	60.5	65.5	55.0
4	Normal	M	81	6	75.6	74.5	75.6	62.3	57.7	64.1
5	Normal	M	77	17	89.7	60.1	76.3	49.7	62.7	62.9
11	Normal	F	48	5	55.9	60.8	78.8	73.5	75.4	64.6
12	Normal	M	73	7	79.2	67.2	65.9	60.4	68.9	61.3
13	Normal	F	73	13.5	88.1	81.9	56.4	63.1	62.7	89.0
14	Normal	M	73	18	63.6	69.4	50.2	72.0	54.6	79.9
15	Normal	M	70	20.5	62.5	70.3	57.2	65.6	60.4	76.5
16	Normal	M	72	23	78.8	72.1	87.3	50.4	62.3	58.7
17	Normal	M	83	28	85.7	80.7	65.6	48.5	57.0	68.9
Normal mean			77	15	73.9	71.1	68.9	60.7	63.7	68.4
Normal SD			12	7	11.2	8.0	11.5	8.0	6.5	10.0
6	AD	M	90	3	68.7	76.1	65.7	72.0	59.0	68.9
7	AD	F	82	6	131.2	101.0	103.9	56.5	73.1	77.1
8	AD	M	75	7	68.4	70.6	63.2	61.8	70.3	74.5
9	AD	M	83	7	87.8	93.5	61.5	63.5	59.0	80.1
10	AD	F	89	20	104.3	100.3	84.7	55.2	60.8	69.6
18	AD	M	73	3	77.1	64.3	58.3	60.6	74.7	83.3
19	AD	M	83	7	85.3	81.1	92.1	56.2	72.5	70.8
20	AD	M	77	7.75	73.3	66.3	63.8	67.4	63.3	81.4
21	AD	M	76	8	79.5	90.8	88.5	69.8	70.2	81.8
22	AD	F	75	8	103.4	97.2	81.1	46.2	60.1	77.3
23	AD	F	78	8	73.4	84.1	66.8	67.9	62.1	81.1
24	AD	M	83	8	89.1	72.3	88.6	59.4	75.3	68.9
25	AD	F	66	9	111.5	112.7	103.7	43.9	41.6	60.8
26	AD	F	94	9	81.9	72.7	80.7	50.4	79.6	72.4
27	AD	M	65	11	104.2	74.9	83.7	48.0	67.3	80.8
28	AD	F	78	24	134.6	102.9	83.8	44.2	66.5	90.9
AD mean			79	9	92.1	85.0	79.4	57.7	66.0	76.2
AD SD			8	5	20.8	14.9	14.6	9.2	9.2	7.4
p[b]			0.54	0.02	0.01	0.01	0.05	0.38	0.46	0.02

[a] FC—frontal cortex, PC—parietal cortex, Cb—cerebellum.
[b] Parameter of statistical significance for the difference between normal and AD mean values.

Table 3
Parameters for individual CSF samples, mean and SD values for controls (1–15A) and AD patients (1–15B) used in this study.

ID	Sex	Age at lumbar puncture (years)	CDR[a]	PIB[b]	Tau[c] (pg/ml)	Ptau181[d] (pg/ml)	CAβ42[e] (pg/ml)	Na (mM)	K (mM)	Gln (μM)	Glu (μM)	Met (μM)
1A	F	66	0	neg	161	28	733	143	2.68	474	4.40	5.46
2A	F	71	0	neg	214	32	913	146	2.82	539	2.88	5.78
3A	M	75	0	neg	258	48	722	144	2.89	559	3.38	6.76
4A	M	66	0	neg	285	44	959	144	2.84	545	2.93	9.41
5A	M	83	0	neg	322	46	860	145	2.78	532	2.76	6.56
6A	F	76	0	neg	624	100	1109	147	2.89	574	2.76	7.74
7A	M	71	0	neg	249	55	844	147	2.86	517	2.71	5.01
8A	F	81	0	neg	330	60	1074	147	2.82	487	2.40	4.81
9A	F	67	0	neg	443	86	1081	147	2.69	511	3.73	4.64
10A	F	69	0	neg	190	41	762	143	2.92	488	3.27	4.77
11A	M	75	0	neg	375	94	736	143	2.72	514	3.70	6.40
12A	F	75	0	neg	400	62	931	149	2.89	532	3.57	5.74
13A	M	70	0	neg	177	39	1056	147	3.06	631	3.59	7.94
14A	F	72	0	neg	214	45	1089	149	2.80	580	3.49	5.70
15A	M	75	0	neg	402	84	1293	144	2.82	774	3.87	10.59
Normal mean		73			310	58	944	146	2.83	550	3.30	6.48
Normal SD		5			125	23	170	2	0.10	74	0.54	1.76
1B	F	73	0[f]	pos	1068	181	326	144	2.72	579	2.96	6.40
2B	F	74	2	pos	963	121	426	150	2.85	560	2.92	6.52
3B	F	82	0.5	pos	929	133	321	146	2.97	574	2.55	7.94
4B	F	65	0.5	pos	481	63	342	149	2.76	544	2.76	5.78
5B	F	81	0.5	–	490	73	391	147	3.03	536	2.74	5.13
6B	M	83	0.5	–	645	76	391	148	2.76	509	2.65	6.31
7B	F	78	0.5	pos	401	58	294	146	2.81	625	2.30	6.76
8B	F	75	0.5	–	578	78	241	144	2.77	485	2.52	5.17
9B	F	82	0[f]	pos	631	88	233	143	2.76	775	3.68	8.15
10B	M	80	0.5	–	569	98	410	146	2.68	645	3.28	7.74
11B	F	80	0[f]	pos	440	74	319	148	2.75	548	3.33	5.58
12B	M	77	0.5	–	307	50	321	147	2.73	538	3.08	6.19
13B	M	74	0.5	–	516	68	202	147	2.77	494	3.16	5.25
14B	F	72	0.5	–	1204	159	393	148	2.73	449	2.93	5.50
15B	F	72	0.5	–	650	165	312	149	2.85	509	3.14	5.54
AD Mean		77			658	99	328	147	2.80	558	2.93	6.26
AD SD		5			262	42	67	2	0.10	79	0.36	1.01
p[g]		0.051			10^{-4}	0.0024	10^{-12}	0.17	0.31	0.79	0.04	0.67

[a] CDR: clinical dementia rating.
[b] PIB: results of [^{11}C]-Pittsburgh B compound positron emission tomography (PET) imaging.
[c] Tau: CSF tau levels.
[d] Ptau181: CSF phospho-tau 181 levels.
[e] CAβ42: levels of Aβ 1–42 peptide in CSF.
[f] Subjects with CDR = 0 are interpreted to be preclinical AD on the basis of positive PIB PET imaging and low CSF Aβ42 levels. Subjects with CDR >0 belong to the AD group.
[g] p: parameter of statistical significance for the difference between control and AD mean values.

extracellular compartment. An increase in the relative extracellular volume in AD brain tissue is also inconsistent with the negligible decrease in tissue K^+ levels in AD frontal cortex samples and the slight increase in tissue K^+ levels in parietal cortex and cerebellum samples. An increase in the relative extracellular volume is expected to result in a significant decrease in K^+ levels since the extracellular $[K^+] \ll$ intracellular $[K^+]$. Based on these lines of reasoning, we conclude that the ion imbalance observed in AD brain tissue is likely to reflect intracellular ion perturbations.

3.2. Comparison of glutamate levels between AD and normal subjects

Estimates of glutamate levels in AD versus control brain have produced contrasting results [28–30]. We measured the glutamate concentration in human brain homogenates and in the CSF. Although slightly higher glutamate levels were observed in all three regions from AD versus control brain samples, the difference did not reach statistical significance (Table 2). In CSF, a modest decrease in glutamate concentration was observed in clinically characterized AD subjects compared to normal controls (Table 3). Differences were not seen in two other metabolites linked to this metabolic hub, methionine and glutamine, in AD versus control cortical samples or in CSF samples, while a significant decrease in methionine was observed in AD cerebellar samples versus controls (Tables 2 and 3).

3.3. Aβ induces Na^+ and K^+ ion imbalances in astrocytes

Astrocytes are the most abundant cells in the brain. To assess whether the ion imbalances seen in brain tissue could be induced by Aβ, we treated primary mouse astrocytes with Aβ 25–35. In response to this treatment, an increase in both intracellular Na^+ and K^+ contents was observed in astrocytes, which was dependent on Aβ concentration (Fig. 1). No changes were observed in the concentrations of these ions in the culture medium. The reverse and inactive Aβ 35–25 peptide had no effect on the cellular Na^+ and K^+ contents (Fig. 1). At 50 μM Aβ 25–35 concentration, where a maximal effect was observed, intracellular Na^+ increased ~1.8- and ~2.6 fold while K^+ increased ~1.4- and ~1.6 fold following acute and repeated Aβ treatment, respectively (Fig. 2a).

The Na^+/K^+ ATPase is primarily responsible for maintaining the Na^+ and K^+ ion gradients across the plasma membrane and the large ion imbalance observed with Aβ treatment suggested impaired activity of this protein. Western blot analysis showed lower Na^+/K^+ ATPase levels in astrocytes that were either acutely or repeatedly treated with Aβ 25–35, with the effect being more significant in the latter case (Fig. 2b, c). The decrease in Na^+/K^+ ATPase expression cannot by itself account for the simultaneous increase in intracellular Na^+ and K^+ contents since inhibition of astrocytic Na^+/K^+ ATPase with ouabain caused increased intracellular Na^+ while concomitantly decreasing intracellular K^+ levels (Fig. 3). Addition of ouabain to Aβ

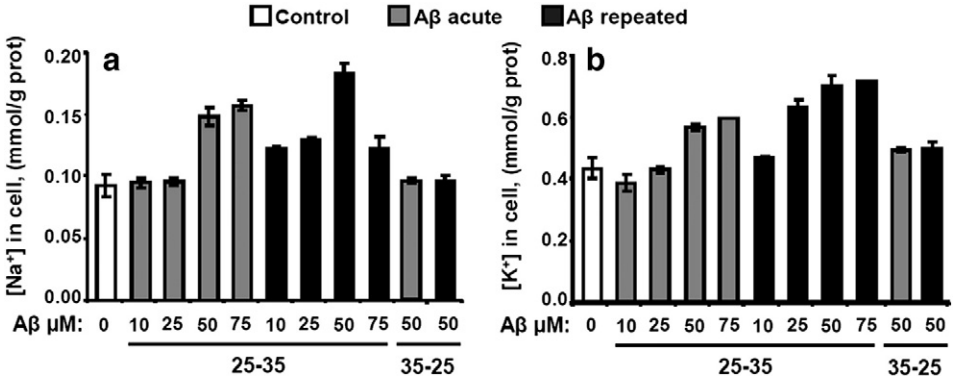

Fig. 1. The effect of different concentrations and forms of Aβ 25–35 on intracellular levels of Na^+ and K^+ in primary mouse astrocytes. Cells were treated acutely (gray bars) or repeatedly (black bars) with different concentrations of Aβ 25–35 or with 50 μM of Aβ 35–25 and intracellular Na^+ (a) and K^+ (b) levels were measured 24 h after acute or the last repeated Aβ treatment as described under Materials and methods. White bars represent data for control *i.e.* untreated cells. Data are representative of 2 independent experiments (with different cell preparations) each performed in triplicate. The bars represent the mean ± SD.

25–35 treated astrocytes selectively increased intracellular Na^+ while K^+ levels decreased to the levels of ouabain treated controls.

Since the transport of glutamate and the cations, Na^+ and K^+, across the plasma membrane is functionally linked, we next examined the effect of Aβ 25–35, if any, on the levels of the astrocytic X_{AG}^- transporters, GLAST and GLT-1, which were reduced with repeated but not acute Aβ 25–35 treatment (Fig. 4).

Treatment of astrocytes with one of the following inhibitors: aspartate β-hydroxamate (for X_{AG}^-), furosemide and bumetanide (for Na/K/Cl co-transport), and dimethyl amiloride (for Na/H exchange), did not significantly influence the cation balance in control cells or affect the cation imbalance in Aβ 25–35 treated cells (data not shown). These results suggest that the corresponding transporters are probably not involved in the ion imbalance induced by Aβ treatment of astrocytes.

The effect of Aβ 25–35 treatment on intracellular Na^+ and K^+ levels is cell specific. While the human astrocytoma cell line, U-87MG, responded like astrocytes to Aβ treatment, the human embryonic kidney epithelial cell line, HEK 293 cells and human T cell leukemia line, Jurkat cells showed no effect (Fig. 5).

We also examined the effects of aggregated Aβ peptides with longer sequences, 1–40 and 1–42, on Na^+ and K^+ levels in cultured mouse primary astrocytes. While Aβ 1–42 did not elicit detectable changes in astrocytic ion balance (data not shown), Aβ 1–40 resulted in a concentration-dependent increase in intracellular Na^+ and K^+ levels (Fig. 6), similar to that observed with Aβ 25–35.

4. Discussion

In this study, we have found differences between Na^+ and K^+ concentrations in postmortem tissue samples from different segments of AD brain compared to controls and this difference is not reflected in CSF Na^+ and K^+ concentrations in these two groups. While ion gradients between cells and extracellular compartments disappear after death and intracellular and extracellular Na^+ and K^+ concentrations equilibrate, the total ion content in a tissue should not be affected because ions are not metabolized and there is no ion exchange with other tissues because of lack of blood circulation. Indeed, the absence of a pronounced correlation between postmortem time of brain collection and tissue ion content (Table 1) confirms that total brain tissue ion content does not change postmortem. A recent study using *in vivo* MRI sodium imaging revealed that hippocampal formations of AD patients had modestly (~10%) higher $[Na^+]$ versus controls [31], which is consistent with our finding of ion imbalance in other brain regions. The increased Na^+ concentration was suggested to be primarily within the intracellular compartment [31]. Since intracellular $[Na^+]$ is >10-fold lower than the extracellular $[Na^+]$, even small changes in a total tissue $[Na^+]$ are expected to be associated with a significant change in intracellular $[Na^+]$.

After excluding the possibility that extracellular ion concentrations contribute to the difference in ion content between normal and AD brain tissue, two other mechanisms were considered: (i) a decrease in the relative cell volume in AD tissue or (ii) an increase in intracellular

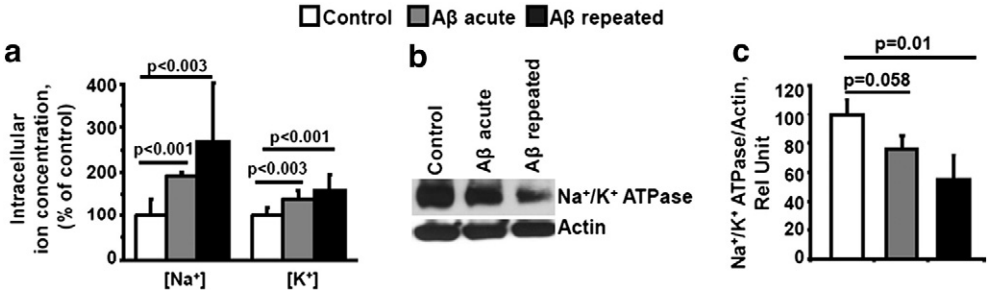

Fig. 2. Changes in ion levels and in the Na^+/K^+ ATPase expression in astrocytes treated with Aβ 25–35. (a) Primary mouse astrocytes were either untreated (white bar) or exposed to acute (gray bar) or repeated (black bar) treatment with Aβ 25–35, and Na^+ and K^+ levels were measured 24 h after acute or the last repeated Aβ treatment as described under Materials and methods. Data are the mean ± SD of 7 independent experiments. (b) Western blot analysis of Na^+/K^+ ATPase α1 subunit in astrocytes treated as in (a). The blot shown is representative of three independent experiments. (c) Quantification of Na^+/K^+ ATPase Western blot data. Vertical bars show the relative expression of Na^+/K^+ ATPase α1 subunit in astrocytes treated as in (a). Data are mean ± SEM obtained in three independent experiments. Numbers above the horizontal lines show statistical significance of the difference between the corresponding vertical bars.

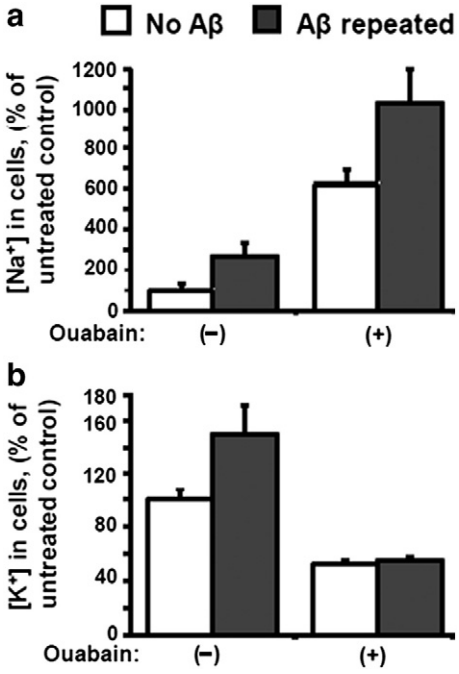

Fig. 3. Effects of ouabain inhibition of Na^+/K^+ ATPase on intracellular cation levels in astrocytes treated with Aβ 25–35. Primary murine astrocytes were cultured without Aβ (white bars) or repeatedly treated with 50 μM Aβ 25–35 (gray bars) as described under Materials and methods. Ouabain was added to the incubation medium to a final concentration of 500 μM at the time of the last treatment with Aβ. Intracellular (a) Na^+ and (b) K^+ levels were measured 24 h later as described under Materials and methods. Data are the mean ± SD (n = 3).

Na concentration in AD tissue. While considering the first mechanism in more detail in the following section, we note that it alone cannot explain an increase in tissue $[Na^+]$ without a corresponding decrease in $[K^+]$ or explain the observed increase in cerebellar $[K^+]$. In the first mechanism *i.e.*, a decrease in the relative cell volume in AD brain tissue with a concomitant increase in the extracellular volume, the total Na^+ concentration is predicted to increase since the extracellular Na^+ concentration is >10-fold higher than its intracellular concentration. The increase in total Na^+ concentration in individual samples should be correlated with a decrease in total tissue K^+ concentration since extracellular K^+ concentration is many-fold lower than its intracellular concentration. To assess this correlation we have employed a mathematical model (Eqs. (1)–(9)). The model predicts that if intracellular and extracellular $[Na^+]$ and $[K^+]$ are constant and only the cell volume fraction in samples vary, then the total tissue K^+ concentration will decrease linearly with increasing total Na^+ concentration (Eqs. (6) and (7)). The corresponding graph (Fig. 7) shows the dependence of total K^+ concentration on total Na^+ concentration as the relative intracellular volume varies between 0 and 100%. Hence, at a theoretical zero intracellular cell volume, Na^+ concentration is high while total K^+ ion is low and corresponds to the extracellular Na^+ and K^+ ion concentrations. Conversely, at a theoretical zero extracellular volume, Na^+ concentration is low while K^+ is high and corresponds to the intracellular Na^+ and $[K^+]$ ion concentrations.

The model predicts that the slope of the graph increases with increasing intracellular cation concentrations (Fig. 7a and b). The lines converge at the same point representing extracellular $[Na^+]$ = 147 mM and $[K^+]$ = 2.8 mM and coincide with our experimentally determined values for $[Na^+]$ and $[K^+]$ in CSF from normal individuals and AD patients. The dotted lines in Fig. 7 correspond to intracellular cation concentrations. As is evident from these plots, the slope is sensitive to increases in intracellular $[Na^+]$ (Fig. 7a) or $[K^+]$ (Fig. 7b).

To assess how our experimentally derived data obtained in brain fit the model we plotted the tissue $[K^+]$ versus tissue $[Na^+]$ determined in each sample (Fig. 8). Data points representing control and AD samples segregate to different areas in the graph. Interestingly, despite the relatively small difference in the average ion concentrations between cerebellar samples from AD versus controls, the data points within each group also tended to segregate (Fig. 8). The linear fit for control (solid lines) and AD (dashed lines) data was obtained by constraining the lines to intersect at the point with coordinates of $[Na^+]$ = 147 mmol/kg tissue and $[K^+]$ = 2.8 mmol/kg tissue. The fitted lines display an excellent correspondence to the experimental data points for the control set implying that individual variations in total $[Na^+]$ and $[K^+]$ (ranging from 50 to 90 mmol/kg tissue $[Na^+]$ and 89.0 to 49 mmol/kg tissue $[K^+]$) result from variations in the fractional intracellular volume (ranging from 0.71 to 0.42). In contrast, the linear fit to the AD data has a significantly higher slope than the fit to the control data in all three brain regions, consistent with increased intracellular cation levels. The experimental data for AD samples exhibit a much greater scatter than the control data. This implies that in the AD samples, an additional source of individual variations exist, which can be ascribed to variations in intracellular cation concentrations.

The linear fit to the control data for frontal cortex yields the following values for parameters representing the constant (A) and slope (B) in Eq. (7): A = 118 mM, B = −0.786. The same values for these parameters can be obtained from Eqs. (8) and (9) using experimentally derived extracellular cation concentrations and at intracellular $[Na^+]$ and $[K^+]$ concentrations of 10 mM and 110 mM respectively. Thus, the linear fit coincides with the modeled plot in Fig. 7, obtained for normal intracellular Na^+ and K^+ concentrations, and supports the presence of normal intracellular cation

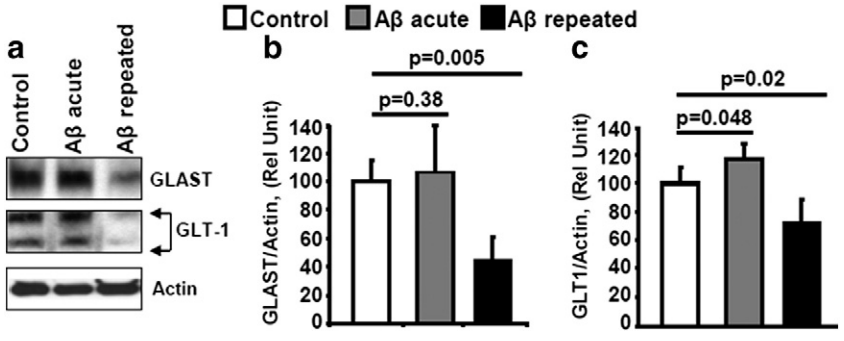

Fig. 4. Changes in expression of excitatory amino acid transporters (GLAST and GLT-1) in astrocytes treated with Aβ 25–35. (a) Primary mouse astrocytes were cultured without treatment, or treated with 50 μM Aβ 25–35 acutely or repeatedly as described under Materials and methods. Western blot analysis of GLAST and GLT-1 levels in the cells was done 24 h after acute or the last repeated Aβ treatment. Quantification of GLAST (b) and GLT-1 (c) Western blot data. The vertical bars represent the GLAST and GLT-1 protein expression levels relative to the untreated controls (white bar) versus acute (gray bar) or repeated (black bar) Aβ-treated cells. For GLT-1, the bars represent the sum of the intensity of the two bands corresponding to the transporter. The Western blot in (a) is representative of two independent experiments and the data in (b) and (c) are mean ± SEM obtained in 2 (GLAST) and 3 (GLT-1) independent experiments. Numbers above the horizontal lines denote the statistical significance of the difference between the corresponding vertical bars.

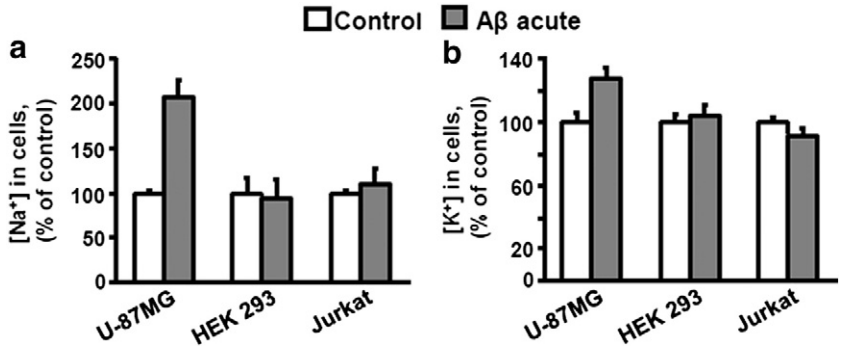

Fig. 5. Cell-specific effect of Aβ 25–35 on intracellular cation levels. Intracellular levels of (a) Na^+ and (b) K^+ were measured in human astrocytoma cells, U-87MG, human embryonic kidney cells, HEK 293 and human T cell leukemia (Jurkat) cells. Ion concentrations were measured in untreated controls (white bars), or in cells acutely treated with 50 μM Aβ 25–35 (gray bars) after 24 h as described under Materials and methods. Cells were cultured and treated with Aβ 25–35 in 6-well plates at a cell density of $1–2\times10^6$ cells/well as described under Materials and methods. Data represent the mean ± SD; n = 4 and 2 for control and Aβ treated U-87GM cells, n = 8 and 4 for control and Aβ treated HEK 293 cells, and n = 4 and 2 for control and Aβ treated Jurkat cells respectively.

concentrations in control samples. The linear fit to the AD frontal cortex data yields the following parameter values: A = 138, B = −0.918. These values can be obtained from Eqs. (8) and (9) at intracellular [Na^+] and [K^+] of 20 mM and 119 mM respectively. The plot of the AD frontal cortex data reveals a significant elevation in intracellular cation concentrations. The estimates for intracellular cation concentrations for all three brain regions are shown in Table 4 and reveal that the difference in cation concentrations between normal and AD brain tissue samples can be explained by a significant (two-fold) increase in intracellular [Na^+] together with a mild (8–15%) increase in intracellular [K^+]. Thus, analysis of our data obtained with postmortem brain samples reveals a significant increase in intracellular Na^+ concentration and a mild increase in K^+ concentration in AD compared to normal brain samples. An obvious limitation of our study is that intracellular Na^+ and K^+ concentrations cannot be measured directly in frozen postmortem brain samples and we are unable to determine whether the ion imbalance affects all or a subset of brain cell types. Direct measurement of Na^+ and K^+ ion concentrations in AD brain samples is precluded by loss of the transmembrane ion gradient in postmortem tissue.

A difference in glutamine and glutamate levels was not observed between normal and AD brain samples (Table 2). It seems unlikely that the use of postmortem tissue obscured possible changes in these amino acid pool sizes since previous reports indicate that glutamine and glutamate levels in brain do not change significantly up to 48 h postmortem [32,33]. On the other hand, methionine increased significantly in postmortem brain tissue from ~10–50 μmol/kg of tissue up to 230 μmol/kg of tissue [32,33]. Hence, the observed difference in methionine levels between normal and AD cerebellum (Table 2) might be related to postmortem methionine accumulation.

We used a cell culture model to assess whether the ion perturbations observed in AD brain samples might be associated with Aβ. Since Aβ induces neuronal death *in vitro*, it precluded their use in the current experimental protocols, which involve a prolonged exposure of cells to Aβ. Instead, we used astrocytes and primarily, the synthetic Aβ 25–35 peptide. While this peptide is generally considered to be unnatural, there is evidence of its presence in AD brain [34,35]. Its greater affordability has resulted in the widespread use of the Aβ 25–35 peptide as a surrogate for the naturally occurring Aβ 1–40/42 peptides, particularly since it often elicits very similar effects [36–41]. We note a further caveat *i.e.*, that while the sequences of the human and murine Aβ 25–35 peptide are identical, the sequences of the longer Aβ 1–40/42 peptides are not, raising some questions about the use of the commercially available human Aβ 1–40/42 peptide sequence in *ex vivo* experiments with murine cells. We note that the Aβ concentration used in our experiments is estimated based on the initial concentration of soluble peptide prior to aggregation. The presence of residual soluble Aβ (monomer, oligomer) in these preparations cannot be ruled out. While the 50 μM Aβ concentration used in our cell culture might be considered to be high, in Alzheimer's disease, cells are exposed to Aβ in soluble and aggregate form over a period of many years. We speculate that prolonged exposure of tissue to lower Aβ concentrations might elicit some of the same effects as short term exposure to higher Aβ concentrations in cell culture experiments.

Interestingly, in our study, the Aβ 1–40 like the Aβ 25–35 peptide induced astrocytic ion imbalance while Aβ 1–42 had no effect. A

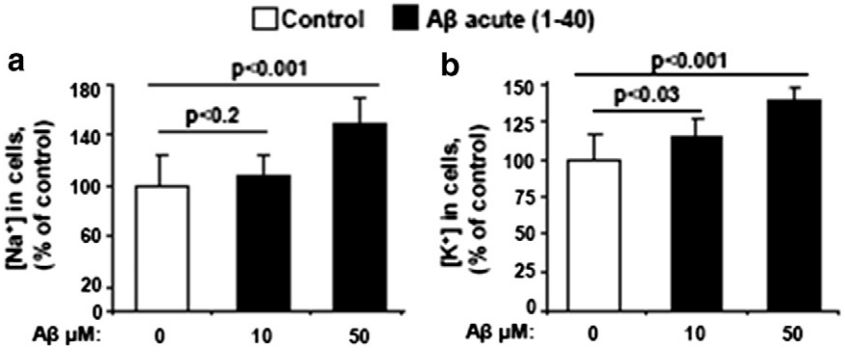

Fig. 6. The effect of Aβ 1–40 on intracellular levels of Na^+ and K^+ in primary mouse astrocytes. Cells were cultured without Aβ treatment (control, white bars) or were acutely treated with 10 or 50 μM of Aβ 1–40 (black bars). Intracellular Na^+ (a) and K^+ (b) levels were measured 24 h after Aβ treatment as described under Materials and methods. Data represent the mean ± SD of two independent experiments each performed in triplicate. Numbers above the horizontal lines show statistical significance of the difference between corresponding vertical bars.

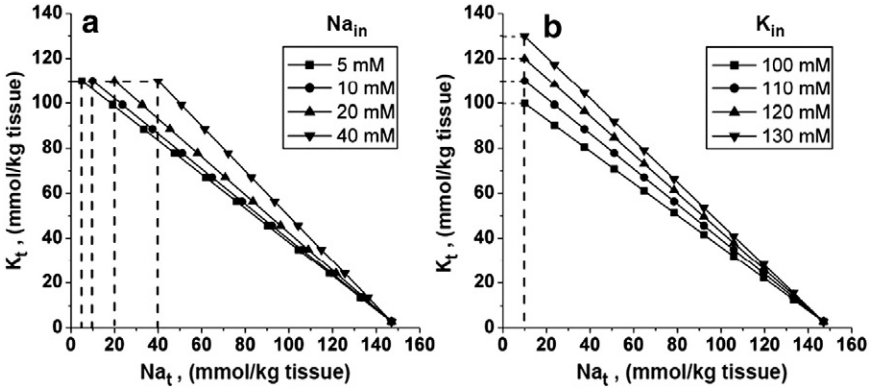

Fig. 7. Modeled dependence of total tissue potassium concentration on total tissue sodium concentration in samples with different relative intracellular volumes. Graphs were plotted using Eqs. (3) and (4) at extracellular $[Na^+]=147$ mM and $[K^+]=2.8$ mM and (a) at intracellular $K_{in}=110$ mM and intracellular Na_{in} of 5, 10, 20, and 40 mM, and (b) at intracellular $Na_{in}=10$ mM and intracellular K_{in} of 100, 110, 120, and 130 mM. Symbols indicate data points with different relative intracellular volumes from 1.0 to 0.0 in 0.1 increments. The point with the lowest K_t value and highest Na_t value corresponds to extracellular $[Na^+]=147$ mM and $[K^+]=2.8$ mM (relative intracellular volume = 0.0). The points with the highest K_t values show intracellular concentrations of Na^+ and K^+ when the relative intracellular volume = 1.0.

difference, albeit in the opposite direction between Aβ 1–40 and Aβ 1–42 has been reported in a study where Aβ 25–35 and Aβ 1–42 caused significant activation of glucose consumption in astrocytes while Aβ 1–40 had no effect [37]. These results demonstrate that even a small difference in the length of the Aβ peptide can be associated with a significant difference in the effects that it elicits warranting caution about results obtained with these peptides. Further, we note that the effects of Aβ 1–40 and Aβ 1–42 on ion concentrations in astrocytes were only studied under conditions of acute treatment. Our studies with Aβ 25–35 show that repeated treatment can elicit significantly larger effects on ion levels than acute treatment (Figs. 1, 2a). Hence, our data do not allow us to exclude the possibility that repeated exposure of brain cells to Aβ 1–42 might also elicit ion imbalance.

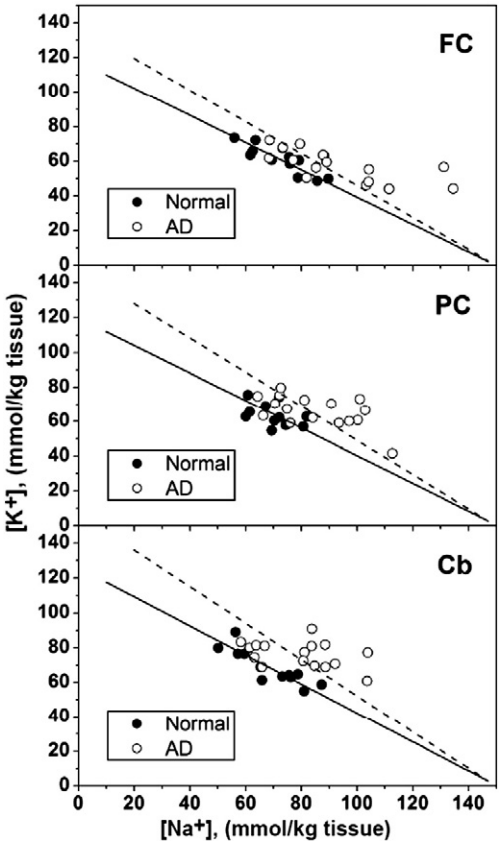

Fig. 8. Comparison of Na^+ and K^+ ion concentrations in brain tissue from AD patients versus matched controls. Na^+ and K^+ ion concentrations were measured in brain homogenates of frontal cortex (FC), parietal cortex (PC) and cerebellum (Cb) from AD (open circles, n = 16) and normal (control) (black circles, n = 12) subjects. Data were normalized to the amount of tissue. Symbols show individual data and the solid and dashed lines represent the linear fits to the control and AD data points, respectively.

Our experiments with cultured astrocytes reveal that both acute and repeated treatments with Aβ 25–35 cause a significant increase in intracellular levels of Na^+ and K^+ that is associated with reduced levels of the Na^+/K^+ ATPase, the Na^+-dependent glutamate transporters, and as previously reported, the glutamate/cystine antiporter [15]. However, the observed ion imbalance (*i.e.* the simultaneous increase in Na^+ and K^+ levels in cells) cannot be explained by a decrease in these transporter levels. Additionally, the Na/K/Cl co-transporter(s) and Na/H exchanger(s) do not appear to be involved in the molecular mechanism of Aβ-induced astrocytic Na^+ and K^+ imbalances.

Aβ is known to influence the permeability of biological membranes [42]. A decrease in astrocytic Kir4.1 (an inward rectifying potassium channel) and the BK channel (a calcium sensitive large conductance potassium channel) has been reported in mouse AD models and in human tissue [43]. While perturbations in the transport and levels of Ca^{2+} and some transition metal ions in AD brain tissue and Aβ treated cells have been studied [42,44,45], changes in Na^+ and K^+ have received little if any attention. To our knowledge, this is the first demonstration that Aβ can cause an imbalance in Na^+ and K^+ levels in astrocytes and the underlying molecular mechanism of this Aβ-induced imbalance warrants further investigation.

Interestingly, the increase in Na^+ and K^+ levels observed in cultured Aβ-treated astrocytes is comparable to the estimated increases in intracellular Na^+ and K^+ concentrations in AD brain tissue, suggesting the possibility that Aβ also causes Na^+ and K^+ imbalances in AD brain cells. Other cell types in brain (neurons, oligodendrocytes and microglia) might also play a role in total Na^+ and K^+ imbalances in AD brain tissue. We note that while Na^+ and K^+ imbalances in AD brain appears to be related to Aβ, our study does not address whether this is a specific feature of AD pathology that is not associated with other diseases, such as schizophrenia, dementia or autism, and merits investigation.

An increase in intracellular ion concentrations is expected to have widespread ramifications on cellular functions ranging from transport to ion conductance and intercellular signaling. An increase in intracellular Na^+ concentration is expected to inhibit the Na^+/Ca^{2+} exchanger leading to accumulation of intracellular Ca^{2+} that, in turn, can stimulate multiple signaling pathways, including cell death initiation [46]. Membrane depolarization caused by a significant ion imbalance in brain is associated with such pathologies as migraine, stroke, and traumatic brain injury [47]. These disturbances are likely to contribute to neuronal

Table 4
Estimates of intracellular N^+ and K^+ concentrations in AD versus control brain samples.[a]

Parameter	Subject	Frontal cortex	Parietal cortex	Cerebellum
A[b] (mM)	Normal	118	120	126
	AD	138	148	157
B[c]	Normal	−0.786	−0.797	−0.838
	AD	−0.918	−0.986	−0.1.049
Na_{in} (mM)	Normal	10	10	10
	AD	20	20	20
K_{in}[d] (mM)	Normal	110	112	118
	AD	119	128	136

[a] The values in this table are obtained from fits to the data shown in Fig. 8.
[b] Parameter A represents a constant in Eq. (7) and is defined in Eq. (8) as described under Materials and methods.
[c] Parameter B represents the slope of the graph in Eq. (7) and is defined in Eq. (9) as described under Materials and methods.
[d] Estimates of intracellular K^+ concentration in control and AD tissue were obtained from the slope of the fitted line using Eq. (9) and assuming that the corresponding intracellular Na^+ concentration is 10 mM and 20 mM for control and AD tissue respectively.

dysfunctions in AD, including dysfunction of intrinsic neuronal excitability [48], and might trigger cell death pathways contributing to the degeneration and atrophy seen in AD brain. A decreased transmembrane Na^+ gradient in astrocytes might be one factor leading to a decrease in glutamate clearance capacity in AD brain. The dramatic decrease in GLAST and GLT-1 protein expression observed in repeatedly Aβ-treated astrocytes if replicated in AD brain, would predict disturbances in synaptic signal transmission. Furthermore, since the transmembrane sodium gradient serves as a driving force for the active transport of many amino acids into cells, dissipation of this gradient would elicit pleiotropic metabolic and physiological dysfunction. On the other hand, the steeper transmembrane K^+ gradient observed in Aβ treated astrocytes if replicated in AD brain, would predict inhibition of uptake of K^+ released by neurons during the repolarization phase of action potentials [16], affecting neuronal electrophysiological activity.

5. Conclusions

Perturbations of Na^+ and K^+ ion pools, critical for electrophysiological activity, membrane transport, and other cellular processes, are largely unstudied in AD. Our demonstration that Aβ application elicits profound increases in both intracellular Na^+ and K^+ concentrations in cultured astrocytes similar to changes in the Na^+ and K^+ pools found in post-mortem tissues from AD brain, suggests aberrations in a fundamental homeostatic mechanism that might be important in the pathophysiology of this neurodegenerative disease. Furthermore, our results demonstrate that while the cerebellum is considered to be unaffected in AD brain, we see evidence for cation imbalance in this region.

Acknowledgements

Support from the National Institutes of Health (5P50 AG008671 to the Michigan Alzheimer's Disease Research Center) is gratefully acknowledged. The CSF samples and associated clinical data were generously provided by the Biomarker Core of the Washington University Alzheimer's Disease Research Center supported by P50AG05681, and P01AG026276 and P01AG03991 from the National Institutes of Health. We gratefully acknowledge Dr. Anne Fagan (University of Washington) for her assistance with providing us information on the CSF samples. This work was supported in part by NIH grants (DK64959 to R.B. and NS34709 to R.K.).

Appendix A. Supplementary data

Supplementary data to this article can be found online at http://dx.doi.org/10.1016/j.bbadis.2012.07.004.

References

[1] M.P. Mattson, Pathways towards and away from Alzheimer's disease, Nature 430 (2004) 631–639.
[2] C.J. Pike, B.J. Cummings, R. Monzavi, C.W. Cotman, Beta-amyloid-induced changes in cultured astrocytes parallel reactive astrocytosis associated with senile plaques in Alzheimer's disease, Neuroscience 63 (1994) 517–531.
[3] D.A. Butterfield, J. Drake, C. Pocernich, A. Castegna, Evidence of oxidative damage in Alzheimer's disease brain: central role for amyloid beta-peptide, Trends Mol. Med. 7 (2001) 548–554.
[4] C.M. Lauderback, J.M. Hackett, F.F. Huang, J.N. Keller, L.I. Szweda, W.R. Markesbery, D.A. Butterfield, The glial glutamate transporter, GLT-1, is oxidatively modified by 4-hydroxy-2-nonenal in the Alzheimer's disease brain: the role of Abeta1–42, J. Neurochem. 78 (2001) 413–416.
[5] N. Hattori, K. Kitagawa, T. Higashida, K. Yagyu, S. Shimohama, T. Wataya, G. Perry, M.A. Smith, C. Inagaki, CI-ATPase and Na+/K(+)-ATPase activities in Alzheimer's disease brains, Neurosci. Lett. 254 (1998) 141–144.
[6] C.A. Dickey, M.N. Gordon, D.M. Wilcock, D.L. Herber, M.J. Freeman, D. Morgan, Dysregulation of Na+/K+ ATPase by amyloid in APP+PS1 transgenic mice, BMC Neurosci. 6 (2005) 7.
[7] S. Fuller, M. Steele, G. Munch, Activated astroglia during chronic inflammation in Alzheimer's disease—Do they neglect their neurosupportive roles? Mutat. Res. 690 (2010) 40–49.
[8] A. Chvatal, M. Anderova, H. Neprasova, I. Prajerova, J. Benesova, O. Butenko, A. Verkhratsky, Pathological potential of astroglia, Physiol. Res. 57 (Suppl. 3) (2008) S101–S110.
[9] A. Meister, M.E. Anderson, Glutathione, Annu. Rev. Biochem. 52 (1983) 711–760.
[10] G.J. McBean, Cerebral cystine uptake: a tale of two transporters, Trends Pharmacol. Sci. 23 (2002) 299–302.
[11] R. Banerjee, V. Vitvitsky, S.K. Garg, The undertow of sulfur metabolism on glutamatergic neurotransmission, Trends Biochem. Sci. 33 (2008) 413–419.
[12] N.C. Danbolt, Glutamate uptake, Prog. Neurobiol. 65 (2001) 1–105.
[13] A. Parpura-Gill, D. Beitz, E. Uemura, The inhibitory effects of beta-amyloid on glutamate and glucose uptakes by cultured astrocytes, Brain Res. 754 (1997) 65–71.
[14] M.E. Harris, Y. Wang, N.W.J. Pedigo, K. Hensley, D.A. Butterfield, J.M. Carney, Amyloid beta peptide (25–35) inhibits Na^+-dependent glutamate uptake in rat hippocampal astrocyte cultures, J. Neurochem. 67 (1996) 277–286.
[15] S.K. Garg, V. Vitvitsky, R. Albin, R. Banerjee, Astrocytic redox remodeling by amyloid beta peptide, Antioxid. Redox Signal. 14 (2011) 2385–2397.
[16] T. Amedee, A. Robert, J.A. Coles, Potassium homeostasis and glial energy metabolism, Glia 21 (1997) 46–55.
[17] V. Alvarez-Maubecin, F. Garcia-Hernandez, J.T. Williams, E.J. Van Bockstaele, Functional coupling between neurons and glia, J. Neurosci. 20 (2000) 4091–4098.
[18] C. Behl, J.B. Davis, R. Lesley, D. Schubert, Hydrogen peroxide mediates amyloid beta protein toxicity, Cell 77 (1994) 817–827.
[19] Anonymous, Consensus recommendations for the postmortem diagnosis of Alzheimer's disease. The National Institute on Aging, and Reagan Institute Working Group on Diagnostic Criteria for the Neuropathological Assessment of Alzheimer's Disease, Neurobiol. Aging 18 (1997) S1–S2.
[20] J.C. Morris, The Clinical Dementia Rating (CDR): current version and scoring rules, Neurology 43 (1993) 2412–2414.
[21] A.M. Fagan, M.A. Mintun, R.H. Mach, S.Y. Lee, C.S. Dence, A.R. Shah, G.N. LaRossa, M.L. Spinner, W.E. Klunk, C.A. Mathis, S.T. DeKosky, J.C. Morris, D.M. Holtzman, Inverse relation between *in vivo* amyloid imaging load and cerebrospinal fluid Abeta42 in humans, Ann. Neurol. 59 (2006) 512–519.
[22] S.K. Garg, R. Banerjee, J. Kipnis, Neuroprotective immunity: T cell-derived glutamate endows astrocytes with a neuroprotective phenotype, J. Immunol. 180 (2008) 3866–3873.
[23] S.K. Garg, J. Kipnis, R. Banerjee, IFN-gamma and IL-4 differentially shape metabolic responses and neuroprotective phenotype of astrocytes, J. Neurochem. 108 (2009) 1155–1166.
[24] C.J. Pike, D. Burdick, A.J. Walencewicz, C.G. Glabe, C.W. Cotman, Neurodegeneration induced by beta-amyloid peptides *in vitro*: the role of peptide assembly state, J. Neurosci. 13 (1993) 1676–1687.
[25] S.K. Garg, Z. Yan, V. Vitvitsky, R. Banerjee, Analysis of sulfur-containing metabolites involved in redox and methionine metabolism, In: D.K. Das (Ed.), Methods in Redox Signaling, Mary Ann Liebert, New Rochelle, 2010, pp. 7–11.
[26] S. Garg, V. Vitvitsky, H.E. Gendelman, R. Banerjee, Monocyte differentiation, activation, and mycobacterial killing are linked to transsulfuration-dependent redox metabolism, J. Biol. Chem. 281 (2006) 38712–38720.
[27] E. Sykova, I. Vorisek, T. Antonova, T. Mazel, M. Meyer-Luehmann, M. Jucker, M. Hajek, M. Ort, J. Bures, Changes in extracellular space size and geometry in APP23 transgenic mice: a model of Alzheimer's disease, Proc. Natl. Acad. Sci. U. S. A. 102 (2005) 479–484.
[28] S. Tilleux, E. Hermans, Neuroinflammation and regulation of glial glutamate uptake in neurological disorders, J. Neurosci. Res. 85 (2007) 2059–2070.
[29] T. Ernst, L. Chang, R. Melchor, C.M. Mehringer, Frontotemporal dementia and early Alzheimer disease: differentiation with frontal lobe H-1 MR spectroscopy, Radiology 203 (1997) 829–836.

[30] R. Rupsingh, M. Borrie, M. Smith, J.L. Wells, R. Bartha, Reduced hippocampal glutamate in Alzheimer disease, Neurobiol. Aging 32 (2011) 802–810.
[31] E.A. Mellon, D.T. Pilkinton, C.M. Clark, M.A. Elliott, W.R. Witschey II, A. Borthakur, R. Reddy, Sodium MR imaging detection of mild Alzheimer disease: preliminary study, AJNR Am. J. Neuroradiol. 30 (2009) 978–984.
[32] T.L. Perry, S. Hansen, K. Berry, C. Mok, D. Lesk, Free amino acids and related compounds in biopsies of human brain, J. Neurochem. 18 (1971) 521–528.
[33] T.L. Perry, S. Hansen, S.S. Gandham, Postmortem changes of amino compounds in human and rat brain, J. Neurochem. 36 (1981) 406–410.
[34] I. Kaneko, K. Morimoto, T. Kubo, Drastic neuronal loss *in vivo* by beta-amyloid racemized at Ser(26) residue: conversion of non-toxic [D-Ser(26)]beta-amyloid 1–40 to toxic and proteinase-resistant fragments, Neuroscience 104 (2001) 1003–1011.
[35] T. Kubo, S. Nishimura, Y. Kumagae, I. Kaneko, *In vivo* conversion of racemized beta-amyloid ([D-Ser 26]A beta 1–40) to truncated and toxic fragments ([D-Ser 26]A beta 25–35/40) and fragment presence in the brains of Alzheimer's patients, J. Neurosci. Res. 70 (2002) 474–483.
[36] J.P. Terranova, J.P. Kan, J.J. Storme, P. Perreaut, G. Le Fur, P. Soubrie, Administration of amyloid beta-peptides in the rat medial septum causes memory deficits: reversal by SR 57746A, a non-peptide neurotrophic compound, Neurosci. Lett. 213 (1996) 79–82.
[37] I. Allaman, M. Gavillet, M. Belanger, T. Laroche, D. Viertl, H.A. Lashuel, P.J. Magistretti, Amyloid-beta aggregates cause alterations of astrocytic metabolic phenotype: impact on neuronal viability, J. Neurosci. 30 (2010) 3326–3338.
[38] Y.G. Kaminsky, M.W. Marlatt, M.A. Smith, E.A. Kosenko, Subcellular and metabolic examination of amyloid-beta peptides in Alzheimer disease pathogenesis: evidence for Abeta(25–35), Exp. Neurol. 221 (2010) 26–37.
[39] X. Chen, J. Zhang, C. Chen, Endocannabinoid 2-arachidonoylglycerol protects neurons against beta-amyloid insults, Neuroscience 178 (2011) 159–168.
[40] W.T. Chiu, S.C. Shen, L.Y. Yang, J.M. Chow, C.Y. Wu, Y.C. Chen, Inhibition of HSP90-dependent telomerase activity in amyloid beta-induced apoptosis of cerebral endothelial cells, J. Cell. Physiol. 226 (2011) 2041–2051.
[41] C. Zussy, A. Brureau, B. Delair, S. Marchal, E. Keller, G. Ixart, G. Naert, J. Meunier, N. Chevallier, T. Maurice, L. Givalois, Time-course and regional analyses of the physiopathological changes induced after cerebral injection of an amyloid beta fragment in rats, Am. J. Pathol. 179 (2011) 315–334.
[42] C.G. Glabe, R. Kayed, Common structure and toxic function of amyloid oligomers implies a common mechanism of pathogenesis, Neurology 66 (2006) S74–S78.
[43] D.M. Wilcock, M.P. Vitek, C.A. Colton, Vascular amyloid alters astrocytic water and potassium channels in mouse models and humans with Alzheimer's disease, Neuroscience 159 (2009) 1055–1069.
[44] C. Supnet, I. Bezprozvanny, The dysregulation of intracellular calcium in Alzheimer disease, Cell Calcium 47 (2010) 183–189.
[45] D.J. Bonda, H.G. Lee, J.A. Blair, X. Zhu, G. Perry, M.A. Smith, Role of metal dyshomeostasis in Alzheimer's disease, Metallomics 3 (2011) 267–270.
[46] D. Bano, P. Nicotera, Ca^{2+} signals and neuronal death in brain ischemia, Stroke 38 (2007) 674–676.
[47] M. Lauritzen, J.P. Dreier, M. Fabricius, J.A. Hartings, R. Graf, A.J. Strong, Clinical relevance of cortical spreading depression in neurological disorders: migraine, malignant stroke, subarachnoid and intracranial hemorrhage, and traumatic brain injury, J. Cereb. Blood Flow Metab. 31 (2011) 17–35.
[48] S.F. Santos, N. Pierrot, J.N. Octave, Network excitability dysfunction in Alzheimer's disease: insights from *in vitro* and *in vivo* models, Rev. Neurosci. 21 (2010) 153–171.